Brain Structure and Function (2025) 230:76
https://doi.org/10.1007/s00429-025-02940-6

ORIGINAL ARTICLE

Neuroimaging and immunofluorescence of the *Pseudopus apodus* brain: unraveling its structural complexity

S. Jiménez[1] · R. Morona[2] · M. J. Ruiz-Fernández[3] · E. Fernández-Valle[4] · D. Castejón[4] · M. I. García-Real[5] · J. González-Soriano[6] · N. Moreno[2]

Received: 24 March 2025 / Accepted: 11 May 2025

Abstract

The present study provides an in-depth neuroanatomical characterization of the brain of *Pseudopus apodus*, combining magnetic resonance imaging (MRI) with histological analysis by immunofluorescence. In the telencephalon, the pallial regions showed distinct anatomical features, including a cortical structure, a dorsal ventricular ridge and the spherical nucleus, but prominent layering patterns, observable on histological slides, were not fully resolved by MRI. Subpallial structures, such as the nucleus accumbens and the basal ganglia, were delineated with histological clarity and further supported by MRI. In the hypothalamic and diencephalic regions, the dense and complex cellular composition made precise delineation of individual nuclei difficult by MRI, in contrast to the histological accuracy, however by MRI the identification of the major tracts running through these domains are clearly identifiable. Mesencephalic and rhombencephalic structures, including the optic tectum, isthmic nuclei, cerebellum, and reticular groups, were systematically described using a combination of histological and MRI techniques. In addition, immunofluorescence analysis of specific markers, such as Calretinin, ChAT, Isl1, Satb1, Serotonin and Tyrosine Hydroxylase, provided higher resolution of functional sub-regions, allowing precise identification of boundaries and facilitating comprehensive regional mapping, showing complex organizational arrangements, both in rostral regions, such as the dorsal ventricular crest, and in caudal regions, within the tegmental and posterior nuclei of the brain, including the ventral tegmental area, substantia nigra and raphe nuclei. These findings establish a robust neuroanatomical framework for *Pseudopus apodus*, contributing significantly to the understanding of reptile brain organization and providing valuable insights into the evolutionary adaptations underlying a limbless lizard neuroanatomy.

Keywords Ophisaurus · Reptiles · Magnetic resonance imaging (MRI) · Brain · Atlas

Abbreviations

Acc	Nucleus accumbens
ac	Anterior commissure
aDVR	Anterior part of the DVR
ap	Area postrema
AT	Area triangularis
BG	Basal ganglia
BON	Basal optic nucleus
bot	Basal optic tract
BST	Bed nucleus of the stria terminalis
Cb	Cerebellum
cc	Central canal
CeA	Central amygdala
Colm	Coclear lateromedial nucleus

✉ J. González-Soriano
juncalgs@vet.ucm.es

✉ N. Moreno
nerea@bio.ucm.es

[1] Achucarro Basque Center for Neuroscience, Scientific Park of the University of the Basque Country (UPV/EHU), 48940 Leioa, Spain

[2] Department of Cell Biology, Faculty of Biological Sciences, Complutense University, Avenida José Antonio Nováis 12, 28040 Madrid, Spain

[3] DB Diagnóstico Por Imagen Veterinario, Calle Tordesillas 4, 28925 Alcorcón, Madrid, Spain

[4] ICTS Bioimagen Complutense, Complutense University, Paseo de Juan XXIII 1, 28040 Madrid, Spain

[5] Department of Animal Medicine and Surgery, Faculty of Veterinary, Complutense University, Avenida Puerta de Hierro s/n, 28040 Madrid, Spain

[6] Department Section of Anatomy and Embryology, Faculty of Veterinary, Complutense University, Avenida Puerta de Hierro s/n, 28040 Madrid, Spain

Published online: 28 May 2025

Coa	Coclear angularis nucleus
Codm	Coclear dorsomedial nucleus
cSC	Cervical levels of the spinal cord
Cx	Cortex
DCN	Dorsal column nucleus
DCx	Dorsal cortex
Di	Diencephalon
DMCx	Dorsomedial cortex
DM	Dorsomedial nucleus
DLA	Dorsolateral amygdala
DLAn	Dorsolateral anterior nucleus
DVR	Dorsal ventricular ridge
fae	External arcuate fibers
fpd	Fasciculus predorsalis
fr	Fasciculus retroflexus
Gc	Central grey
Hb	Habenula
H	Hypothalamus
IIIv	Third ventricle
Igl	Internal granular layer
Ip	Interpeduncular neuropil
Ipn	Interpeduncular nucleus
Is	Isthmus
Iss	Superficial isthmic nucleus
Isp	Posterior isthmic nucleus
Ism	Medial isthmic nucleus
IV	Troclear nucleus
IVm	Motor troclear nucleus
IVv	Fourth ventricle
IX	Lamina of the spinal cord
LCx	Lateral cortex
Lc	Locus ceruleus
LDT	Laterodorsal tegmental nucleus
LF	Lateral funiculus of the spinal cord
Ma	Mammillary area
MCx	Medial cortex
Mesen	Mesencephalon
ml	Mitral cell layer of the olfactory bulb
MLF	Medial longitudinal fasciculus
Nsol	Nucleus of the solitary tract
NS	Nucleus sphericus
nCbm	Nucleus cerebellosus medialis
OB	Olfactory bulb
oc	Optic chiasm
on	Optic nerve
OT	Optic tectum
ot	Optic tract
Pa	Paraventricular nucleus of hypothalamus
PB	Parabrachial area
pc	Posterior commissure
pDVR	Posterior part of the DVR
pi	Pineal gland
PM	Profound mesencephalic area
PO	Preoptic area
PTc	Pretectum
PTh	Prethalamus
R	Red nucleus
r0	Isthmus
r1–r11	Rhombomeres 1 to 11
Ras	Raphe superior
Rasm	Raphe superior medial
Rhom	Rhombencephalon
Ri	Inferior reticular nucleus
Ris	Istmic reticular nucleus
Rm	Median reticular nucleus
Rt	Nucleus rotundus
S	Septum
sac	Stratum album centrale
sc	Spinal cord
SC	Suprachiasmatic nucleus
Sd	Dorsal septum
sgc	Stratum griseum centrale
sgfp	Stratum griseum et fibrosum periventriculare
sgfsi	Inner part of stratum griseum fibrosum et superficiale
sgfse	External part of stratum griseum fibrosum et superficiale
SN	Substantia nigra
Sm	Medial septum
so	Stratum opticum
sol	Solitary tract
Str	Striatum
Sv	Ventral septum
Tegm	Tegmentum
Tel	Telencephalon
Th	Thalamus
TSC	Central nucleus of the torus semicircularis
TSL	Laminar nucleus of the torus semicircularis
Tub	Tuberal area of the hypothalamus
Tor	Torus
Torc	Torus caudalis
v	Ventricle
Vd	Descending nucleus of the trigeminal tract
vesp	Trigeminoespinal tract
Vevl	Nucleus vestibularis ventrolateralis
Vevm	Nucleus vestibularis ventromedialis
Vllmd	Facial nucleus medio-dorsal part
Vl	Trochear nucleus
VF	Ventral funiculus
vh	Ventral horn of the spinal cord
Vm	Trigeminal motor nucleus
VTA	Ventral tegmental area
V-VI	Layers of the spinal cord
vz	Ventricular zone
X	Periependimary layer of the spinal cord

VII-VIII	Layers of the spinal cord
Zi	Zona incerta

Introduction

Magnetic resonance imaging (MRI) is a very powerful and widely used technique in medical studies, relatively incipient in fields such as evolutionary neurobiology or paleobiology, although in recent years interest has grown due to its wide applicability as a non-invasive technique permitting the study of models that would otherwise be inaccessible (Vickery et al. 2020; Oelschläger et al. 2007; Mietchen et al. 2007; Hoffmann et al. 2014). And thus, recently there have been significant advances in MRI studies in animals not traditionally used in neuroscience research. In particular, an increasing number of brain atlas of reptile species have been published in recent years (Hoops et al. 2018, 2021; Pritz et al. 2020; Behroozi et al. 2018; Jiménez et al. 2024).

Among reptiles, and specifically lizards, the family Anguidae is commonly known as glass lizards or glass snakes, as it includes species that are often limbless, but anatomically they can be identified as lizards by the characteristic shape of their heads, the presence of eyelids and the external openings of their ears. It comprises approximately 20 recognized species, originating in North America, dispersing to Europe and spreading to Asia during the Oligocene (Macey et al. 1999). In particular, the European glass lizard, *Pseudopus apodus* (Pallas 1775), is the largest legless lizard in Europe (Arnold and Ovenden 2002; Obst 1981), and the only extant specie with a distribution spanning Asia Minor, Central Asia, southeastern Europe, and the Balkans (Jandzik et al. 2018). Fossil evidence indicates that *Pseudopus apodus* has been present in the region since the early Miocene (Klembara 2015). Molecular analyses have confirmed the existence of two subspecies (Obst 1978, 1981), closely related to North American anguines such as *Ophisaurus*, but it forms a monophyletic clade with the genus *Anguis* (Macey et al. 1999; Pyron et al. 2013).

Research on the brain of *Pseudopus apodus* is almost non-existent, but there are studies on the closely related genus Ophisaurus (Kulikov and Safarov 1969; Ivazov and Belekhova 1982; Ivazov 1983; Belekhova and Ivazov 1983; Belekhova and Nemova 1987, 1988; Belekhova 1990, 1991; Pierre et al. 1990; Rio et al. 1992) and with which many comparisons can be inferred, suggesting that its neuroanatomical organization is most likely related to its ecological role as a generalist diurnal terrestrial predator (Rifai et al. 2005), highly dependent on sensory information for navigation and foraging. *Pseudopus apodus* shows diverse habitat preferences depending on its geographic range and, although sexual dimorphism is not prominent, it has been observed in certain populations (Çiçek et al. 2014; Kukushkin and Dovgal 2018). Therefore, the brain of *Pseudopus apodus* consists of the forebrain, involved in olfactory processing, spatial navigation and social behavior; the midbrain, for visual and auditory processing, crucial for its diurnal lifestyle; and the hindbrain, which controls basic motor and autonomic functions and coordinates the undulating locomotion necessary for terrestrial movement.

Noticeably, the lack of in-depth neuroanatomical studies and MRI techniques represent an important gap in our knowledge of this species, especially considering the ecological data available. Comparison of these data with neuroanatomical information would provide valuable insights into anatomical-functional relationships and its evolutionary position within reptiles, particularly considering that it is a legless lizard. Therefore, the main objective of the present study is to provide a detailed analysis of the brain of this model, through the combined use of MRI and immunofluorescence identification of conserved markers, complementing the recent study on its anatomy (García-Real et al. 2025) and following in the wake of previous neuroanatomical data recently published in reptiles (Jiménez et al. 2024). Thus, they contribute to complete this important framework of information for understanding this evolutionary node.

Materials and methods

Animals and tissue preparation

For the present study, we used 4 healthy adult *Pseudopus apodus* individuals (2 males and 2 females), homogeneous in size (with an average size of 100 cm) between 5 and 10 years of age. The regulations and laws established by European Union (2010/63/EU) and Spain (Royal Decree 118/2021) for care and handling of animals in research has been followed and the approval from the Ethic committee of the Complutense University (O.H. (CEA)- UCM-NP0409032022-2022).

By intraperitoneal injection (sodium pentobarbital; 50–100 mg/kg, Normon Labs, Madrid, Spain) the animals were anesthetized and perfused transcardially (4% paraformaldehyde in a 0.1 M phosphate buffer, pH 7.4) and the brains removed from the skull.

MRI ex vivo

MRI studies were performed in two brains at BioImaC (ICTS BioImagen Complutense, Madrid, Spain), node of the ICTS ReDIB (https://www.redib.net/). A 4.7-teslas MRI scanner [Biospec 47/40; Bruker BioSpin GmbH, Ettlingen, Germany], equipped with a 6-cm gradient system that provides a gradient strength of 900 mT/m, was used for ex vivo studies. The brains were drained and immersed

in a proton-free susceptibility-matching fluid, Fluorinert® FC-40 (Sigma-Aldrich, Saint Louis, MO, USA) and placed inside a 3.5-cm volume radiofrequency coil. The MRI experiment consisted of three-dimensional T2 horizontal weighted images (T2 WI) used for identification of brain structures. Three-dimensional T2 WI were obtained using a rapid acquisition with relaxation enhancement (RARE) sequence, with a repetition time (TR) = 2622 s, echo train length = 4, interecho interval = 35 ms (resulting in an effective echo time (TE) = 82 ms), number of averages = 4, field of view (FOV) = 30 × 7.5 × 7.5 mm3. The acquired matrix size was 384 × 96 × 96. The raw data were zero-filled to get a reconstructed matrix size of 512 × 128 × 128 (resolution in each direction 59 µm) and the total acquisition time ~ 6 h 42 min. Then horizontal images were reconstructed in axial, sagittal and coronal orientations with an isotropic resolution of 25 µm.

Histological and immunolabeling experiments and controls

Two brains were subjected to the same experimental procedure of MRI followed by histological analysis. The other two brains were directly processed to immunohistochemistry.

For Nissl staining, brain sections were immersed in cresyl violet, followed by differentiation and dehydration with alcohol for optimal visualization of neuronal nuclei. Additionally, we performed immunohistochemistry (refer to Table 1 for commercial specifications, immunogen details, and antibody dilutions) for single and combined detection of Calretinin (CR), Choline Acetyltransferase (ChaT), Islet-1 (Isl1), Special AT-rich sequence-binding protein 1 (Satb1), Serotonin (5-HT) and Tyrosine Hydroxylase (TH).

Immunofluorescence co-labeling was conducted on free-floating sections obtained with a freezing microtome (30–40 µm thickness) in the transverse or sagittal planes. The procedure was as follows: (1) Primary antibody incubation was carried out for 48 h at 4 °C (refer to Table 1 for antibody specifics); (2) Secondary antibody incubation, based on the species of the primary antibody, was performed for 90 min at room temperature using a 1:500 dilution. The secondary antibodies used were Alexa 594-conjugated goat anti-rabbit (red fluorescence; Molecular Probes, Eugene, OR; catalog #A-11037) and Alexa 488-conjugated goat anti-mouse (green fluorescence; Molecular Probes; catalog #A-21042). Following incubation, the sections were mounted on glass slides and coverslipped with fluorescence mounting medium containing 1.5 µg/ml 4′,6-diamidino-2-phenylindole (DAPI) for DNA counterstaining (Santa Cruz; catalog #SC-24941).

Control experiments for the immunohistochemical procedures included the omission of either the primary or secondary antibody, as well as incubating selected sections with preimmune mouse or rabbit serum instead of of the primary antibody. No residual staining was observed in any control section. In addition, previous studies analyzing the specificity of the antibodies used have shown that they exhibit specificity in the reptile species tested and/or comparable and coherent expression patterns (Medina et al. 1994; Guirado et al. 1999b; Morona et al. 2006; Moreno et al. 2010, 2012; Jiménez et al. 2025).

Analysis of photomicrographies

The sections were analyzed with an Olympus BX51 microscope equipped for fluorescence and photographed with a digital camera (Olympus DP74). Contrast and brightness of the photomicrographs were adjusted in Adobe Photoshop CS6 (Adobe Systems, San Jose, CA) and figures were mounted in Canvas X (ACD Systems, Canada).

Table 1 List of primary and secondary antibodies used, immunogen, commercial supplier and dilution

Name	Immunogen	Commercial supplier	Dilution
CB	E-coli-produced recombinant rat calbindin D-28 k	Polyclonal rabbit anti-calbindin D-28; Swant, Bellinzona, Switzerland. Catalog No. CB-38a	1:500
ChaT	Developmental Studies Hybridoma Bank, mouse monoclonal, Cat# 40.2D6	Mouse monoclonal, Developmental Studies Hybridoma Bank. Catalog No. 40.2D6	1:100
CR	E-coli-produced recombinant human calretinin	Polyclonal rabbit anti-calretinin; Swant, Bellinzona, Switzer- land. Catalog No. 7699/4	1:1000
Isl1	Amino acids 247–349 at the C-terminus of rat Islet 1	Mouse monoclonal, Developmental Studies Hybridoma Bank. Catalog No. 40.2D6	1:500
Satb1	Amino acids 241–310 located in the internal region of human-origin SATB1	Monoclonal mouse, Santa Cruz. Catalog No. sc-376096	1:100
Ser (5-HT)	Serotonin coupled to BSA with paraformaldehyde	Polyclonal rabbit anti-5-HT, Immunostar. Catalog No: 20080	1:1000
TH	TH purified from rat pheochromocytoma cells	Mouse monoclonal, ImmunoStar. Catalog No. P22941	1:1000

Results

Figure 1 illustrates the appearance of the *Pseudopus apodus* study model (Fig. 1A), along with dorsal (Fig. 1B), ventral (Fig. 1C), and lateral (Fig. 1E) views of the intact brain, as well as the three-dimensional reconstruction of the brain following MRI scans in the dorsal (Fig. 1D) and sagittal (Fig. 1F) planes. The white lines in Fig. 1E show the approximate section levels observed in the transverse slices presented in Figs. 2, 3 and 4. Transverse sections depicting the rostrocaudal organization of the adult *P. apodus* brain, stained with Nissl for nuclear visualization, are shown in Figs. 2 and 3. Corresponding rostrocaudal transverse MRI images were selected at similar levels (Fig. 4). The same assay has also been visualized in sagittal and dorsal planes (Fig. 4). Finally, for the specific identification of nuclei and regions in the *P. apodus* brain, the expression of specific markers (see Table 1) has been analyzed (Figs. 6, 7, 8 and 9). The anatomical description will be conducted in a topographical rostrocaudal sequence just for a ready comparison with previous studies and following previous maps and descriptions of reptiles (specifically of lizards), due to the limited number of studies on the brain of this species. This is remarkable in the description of the telencephalon, but the interpretation of the results is always considered within the prosomeric paradigm. Furthermore, the discrepancies observed in any region or nuclei, in comparison to what has been described in reptiles in general, or in lizards in particular, will be commented in the discussion section.

At rostral levels of the telencephalon, using Nissl nuclear staining (Fig. 2A–I) the topographical dorsal region showed a layered organization known as the pallium. These layers form the cortical areas (medial: MCx, dorsomedial: DMCx, dorsal: DCx, and lateral: LCx, see Fig. 3A–C for a more detailed view), that cannot be identified through MRI (Fig. 4A–I). The most rostral levels of the pallial region coexists with a structure identified in lizards as the anterior dorsal ventricular ridge (aDVR). This nucleus, which lacks laminar organization, is adjacent to the laminated domain of the lateral cortex (Figs. 2B–D, 3A, B). This particular area in lizards is confined to anterior regions, but not in turtles (Jiménez et al. 2024). On the other hand, in the subpallial region, specifically at the most ventral tip, close to the lateral ventricle, another cellular clustering is observed, and due to its location, it is suggested to correspond to the accumbens nucleus (Acc; Fig. 2B, C). This nucleus is also visible through MRI (Fig. 4B, C). At the pallial levels where the aDVR disappears, it is substituted caudally by its most posterior part (pDVR). It represents the most prominent pallial structure in sauropsids (birds and reptiles), extending rostrocaudally (Fig. 2E, F). The pDVR is clearly identifiable through MRI in transverse sections (Fig. 4D-F), as well as in sagittal and dorsal sections (Fig. 5A, B, D). Further caudally, the position of the DVR is occupied by a structure organized in concentric layers, identified as the spherical nucleus (NS; Figs. 2G, H, 3C). Although the layers are not identifiable through MRI, the nucleus itself is visible (Fig. 4H, I). Ventrally at this level, in the subpallium, the basal ganglia (BG) are identified by Nissl staining (Fig. 2D–F) and by MRI (Fig. 4C–F). At the level of the anterior commissure (ac), in the caudal regions of the telencephalon, when the optic recess and optic chiasm (oc) become visible, the MRI allows a clear view of both tracts, as well as the extension of the oc (Figs. 2G, 4G), and the optic tract (ot; Figs. 2H, 3D, 4I). In the hypothalamic (H) and diencephalic regions, the high density of the cellular populations complicates the precise identification of specific nuclei without the use of specialized staining for these areas (compares Figs. 2H, I and 4H–L; Fig. 3D, E). However, MRI allows the precise recognition and mapping of the ventricular system's extent at these levels, which facilitates a clear identification of the anatomical territories. Caudally, the optic tectum (OT) in the mesencephalon is clearly visible, since it is highly developed and exhibits a well-defined laminar organization in this model (Figs. 2J–M, 3F). However, with the MRI technology used in this study, lamination in this region is only weakly suggested (Fig. 4L–P). In the mesencephalic tegmentum (Tegm), both nuclear staining (Figs. 2K–M, 3F′) and MRI (Fig. 4M–O) do not provide sufficient resolution to identify specific nuclei, although they allow for the identification of the major fiber tracts passing through this structure, similarly to what is observed in the rhombencephalic region (Figs. 2M–R, 4Q–Z). In the rostral rhombencephalon (Rhom), the cerebellum (Cb) is clearly identifiable (Figs. 2N, O, 4R, S), distinctly positioned, covering the fourth ventricle, as evidenced in the sagittal and dorsal MRI (Fig. 5A, B, D). This structure exhibits a heterogeneous organization in terms of cellular density, with a granular layer densely populated, clearly visible by MRI (Figs. 2O, 4S).To support this anatomical identification (Figs. 2, 3, 4 and 5), the expression patterns of key markers were analyzed using immunofluorescence (Figs. 6, 7, 8 and 9). These markers, previously described in the brains of other reptiles, allow a consistent identification of the regions outlined and their comparison with previously reported data.

At topographical more rostral levels, in the olfactory bulb (OB), well-organized layers are observed, containing CR-immunoreactive (-ir) cells that alternate with cells expressing TH (Fig. 6A). Caudally, both CR (Fig. 6B) and TH expression (Fig. 6C) persist in the rostral subpallium, which is essential for identifying the septum (S) and, therefore, delineating the boundary with the medial cortical region and

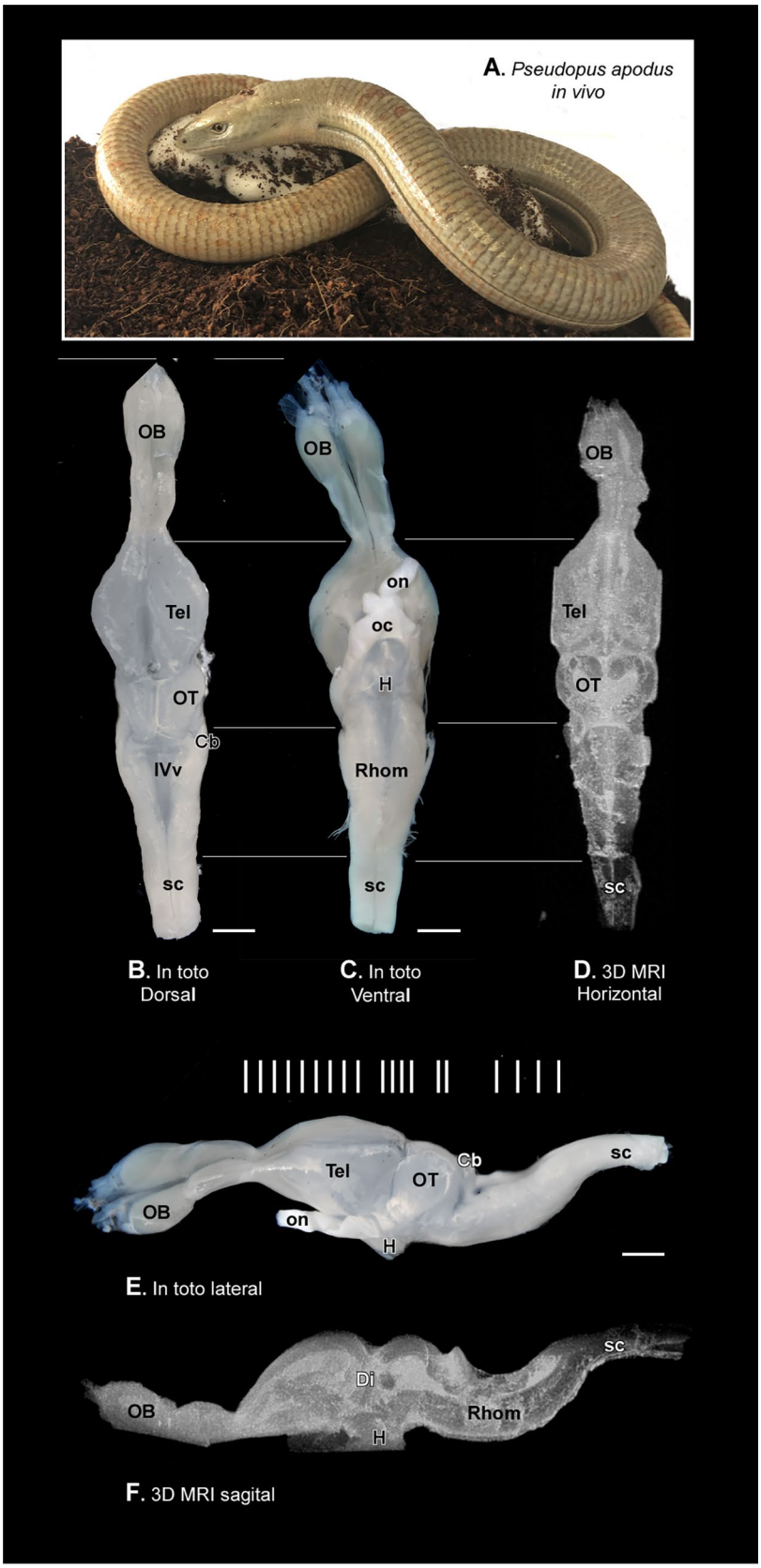

Fig. 1 *Pseudopus apodus* images: in vivo photograph and anatomical views of the brain through 3D MRI reconstruction. **A** In vivo photograph of *Pseudopus apodus*. **B** Dorsal view, **C** ventral view, and **E** lateral view of the brain of *Pseudopus apodus*. **D**, **F** The 3D MRI reconstruction in dorsal and sagittal views, respectively. Scale bar = 1 mm. See the list of abbreviations for further reference

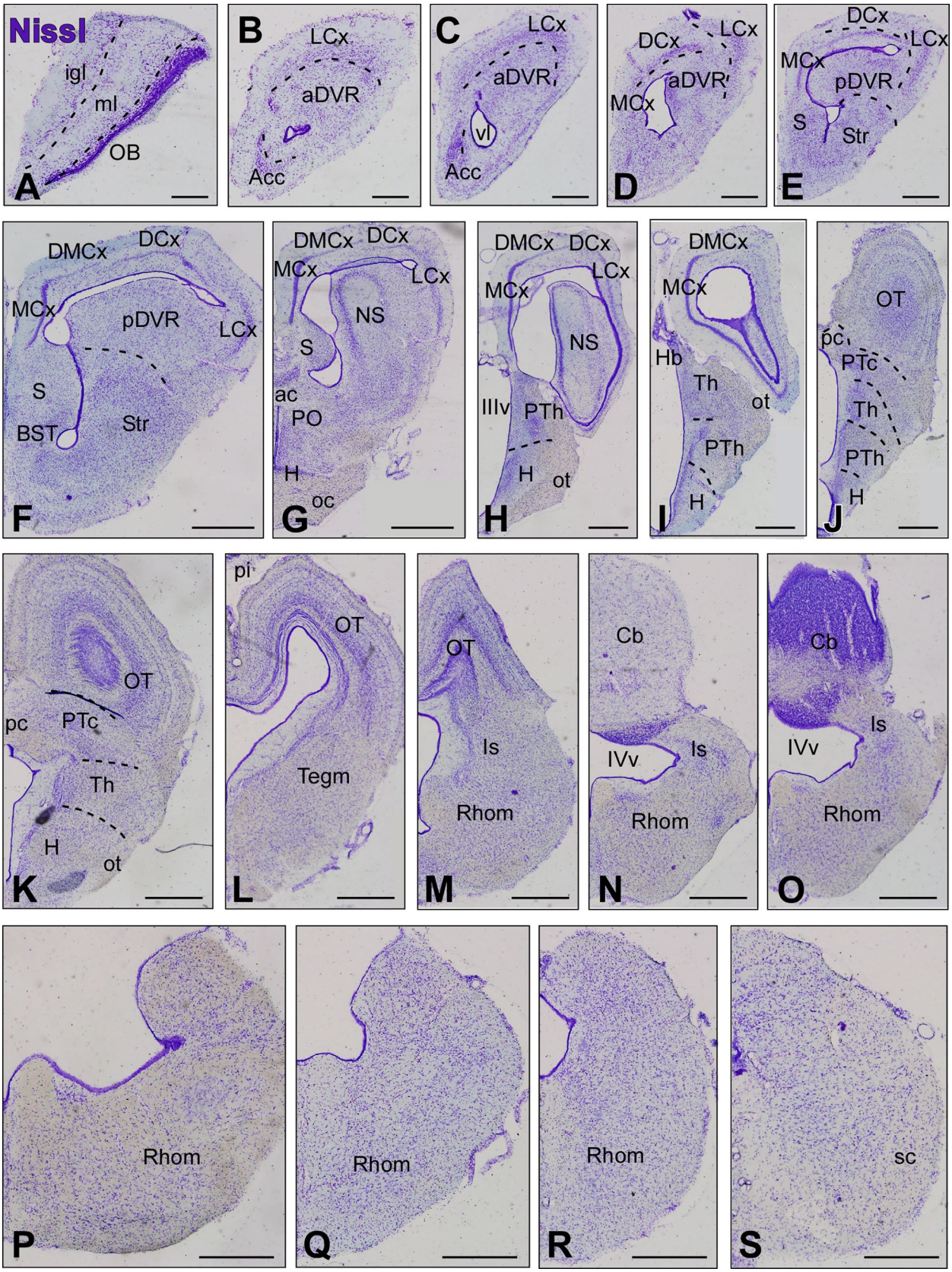

Fig. 2 Nissl-stained sections of the *Pseudopus apodus* brain. Transversal Nissl-stained sections of the brain of *Pseudopus apodus*, from the rostral olfactory bulb (A) to the rostral spinal cord (S). Scale bar = 500 µm. See the list of abbreviations for reference

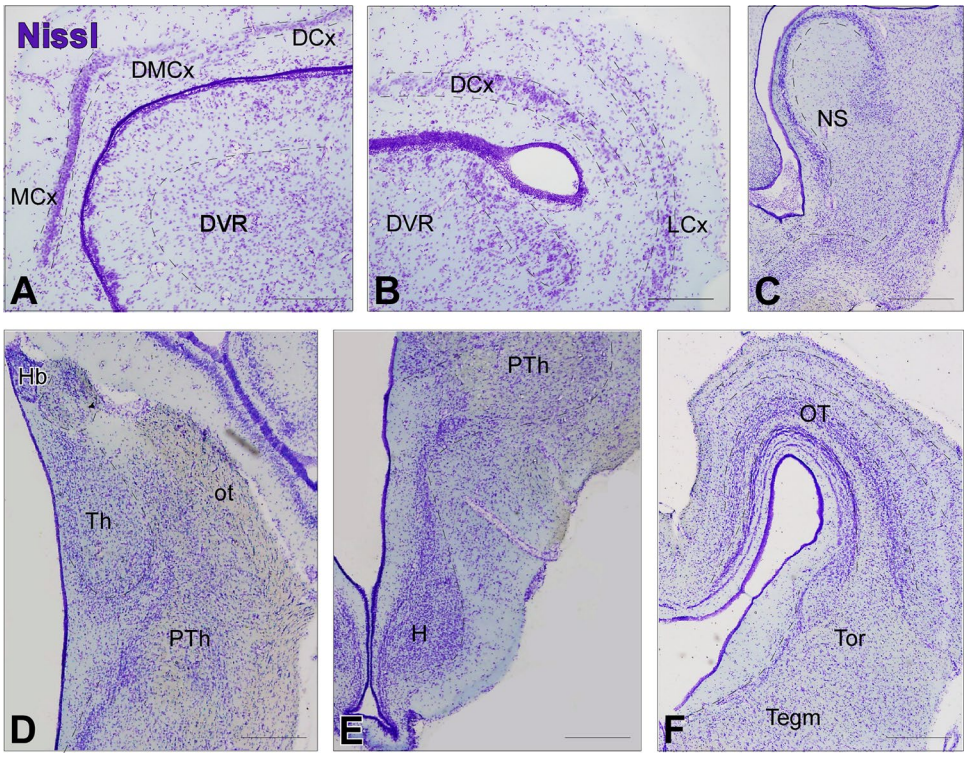

Fig. 3 Enlarged view of specific regions highlighted in Fig. 2. Transverse Nissl-stained brain sections of *Pseudopus apodus* showing detailed views of the pallial (**A**–**C**), thalamic (**D**), hypothalamic (**E**), and tectal (**F**) regions. Scale bar = 200 µm. See the list of abbreviations for reference

ventrally with the Acc (Fig. 6D). At similar levels, in the pallial region, Satb1 expression (Fig. 6E–G) clearly defines the LCx, and aDVR, showing significant expression close to the ventricle. At more medial levels, the DMCx appears to have significant TH innervation, supporting its delineation (Fig. 6H). Furthermore, its subpallial innervation (Fig. 6I, J), along with CR expression (Fig. 6K), allows the identification of different subpallial populations, particularly in the medial region, where dorsoventral septal nuclei are identified with differential TH/CR expression, such as in the dorsal and medial portions (Sd; Sm; Fig. 6L). Further caudally, both expressions remain intense in the subpallium (Fig. 6M, N, S), as confirmed by comparison with Isl1 expression (Fig. 6O). At these levels, TH fibers also reach the region of the dorsolateral amygdala (DLA) closest to the ventricle (Fig. 6M). Similarly, the NS exhibits a notable TH innervation (Fig. 6S), although it does not show Satb1 expression (Fig. 6R). In the subpallium, TH staining clearly defines, at these levels, the dorsal portion of the septum (Sd; Fig. 6S), which is identified along with the ventral septum (Sv) and the BST and the central amygdala (CeA) by the expression of Isl1 (Fig. 6O, T). In Fig. 7, the specific expression of Satb1 defines the most anterior portion of the hypothalamus the paraventricular area (Pa) (Fig. 7A), distinct from the also positive telencephalic preoptic zone (PO) that in MRI images cannot be defined (Fig. 4A, G–I). Noticeably the optic chiasm in *Pseudopus* is massive and extends along preoptic and hypothalamic areas as seen in sagittal sections (Fig. 5) The anatomical regionalization of these two territories, telencephalic vs. hypothalamic, is achieved through the combination of TH and CR expression (Fig. 7B), and the additional expression of Isl1 further enables the identification of the hypothalamic-prethalamic boundary (Fig. 7C, D). The Isl1 pattern further supports the similarity with the Nissl-stained sections (Figs. 2H, 3E), demonstrating a peri/paraventricular hypothalamic organization. Caudally, the habenula is located in the dorsal portion (Fig. 7E–J). This structure shows CR-immunoreactive (CR-ir) cells in the dorsal part of the retroflex fasciculus, positive for TH (Fig. 7E, J), as well as Isl1-ir cells (Fig. 7F) and serotonergic innervation in the medial portion (see the arrowhead in Fig. 7G–I). The combination with cholinergic labeling (absent in this territory) confirms the localization of the medial portion of the habenula (Hb; Fig. 7G–I). In the thalamic region, serotonergic and TH innervation identify the hypothalamic-thalamic tract (Fig. 7G, K; previously observed by MRI, see Fig. 4J). Additionally, the zona incerta (ZI) is identified by intermingled CR-ir and TH-ir cells (see empty arrow in Fig. 7J, K). Finally, the intense CR expression in the thalamus, combined with TH, facilitates the identification of its boundary with the basal mammillary region of the hypothalamus (Ma, Fig. 7L, M). In the midbrain, the OT dorsally and the tegmentum (ventrally) are clearly identifiable by MRI, but other rostrocaudal or dorsoventral subdivisions are not observed. Immunohistochemical techniques revealed a clear alar region with the optic tectum that

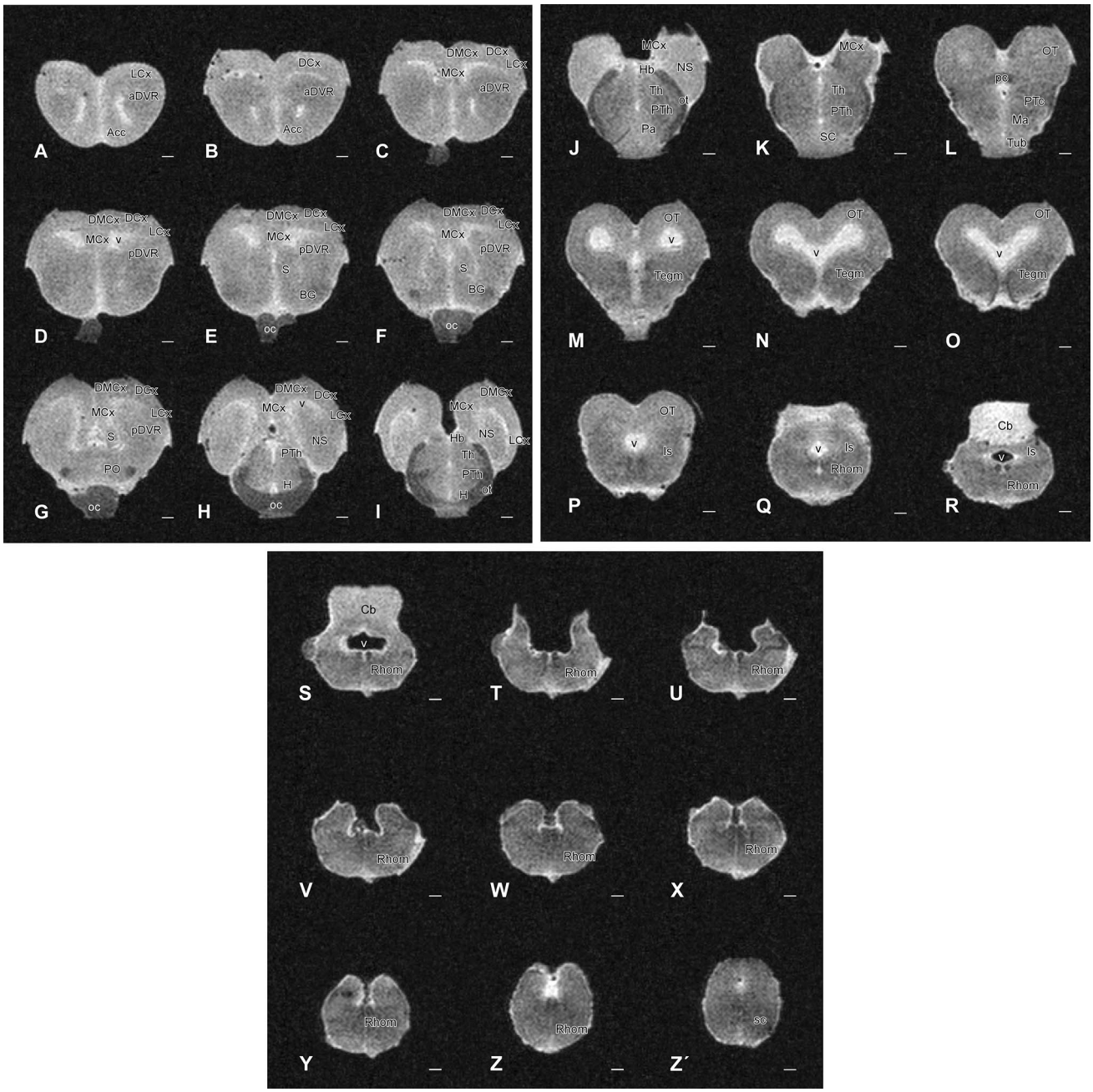

Fig. 4 Rostral-caudal transversal sections of the *Pseudopus apodus* brain from 3D MRI. Transversal sections of the *Pseudopus apodus* brain, organized rostrocaudally, with the main brain regions indicated. Scale bar = 500 µm. See the list of abbreviations for reference

continued with the toral region that included the TH-ir zone corresponding to the torus laminaris (TSL; Fig. 8H), as well as CR-ir subpopulations of the torus semicircularis centralis (TSC) and the profundus mesencephali nucleus (PM). The basal tegmentum included a medial band that using TH labeling, revealed the most noticeable populations identified as the ventral tegmental area (VTA; Fig. 8E, F, H) and the substantia nigra (SN; Fig. 8A, B, D, H). The combination with CR-ir reveals additional distinct cell groups as the basal optic tract root nucleus (BON), and the red nucleus (R; Fig. 8C). Noticeably, the TH immunofluorescence combined with CB highlights the extent and distribution of the tectal layers (Fig. 8G), where fibers were marked in the periventricular gray layer (SGP) and the optic stratum (SO). Additionally, immunofluorescence with CB labeled both cells and fibers in the central gray stratum (sgc), the superficial external fibrous gray stratum (sgfs), and the stratum album centrale (sac). Caudally, at the isthmic region ChAT-ir cells

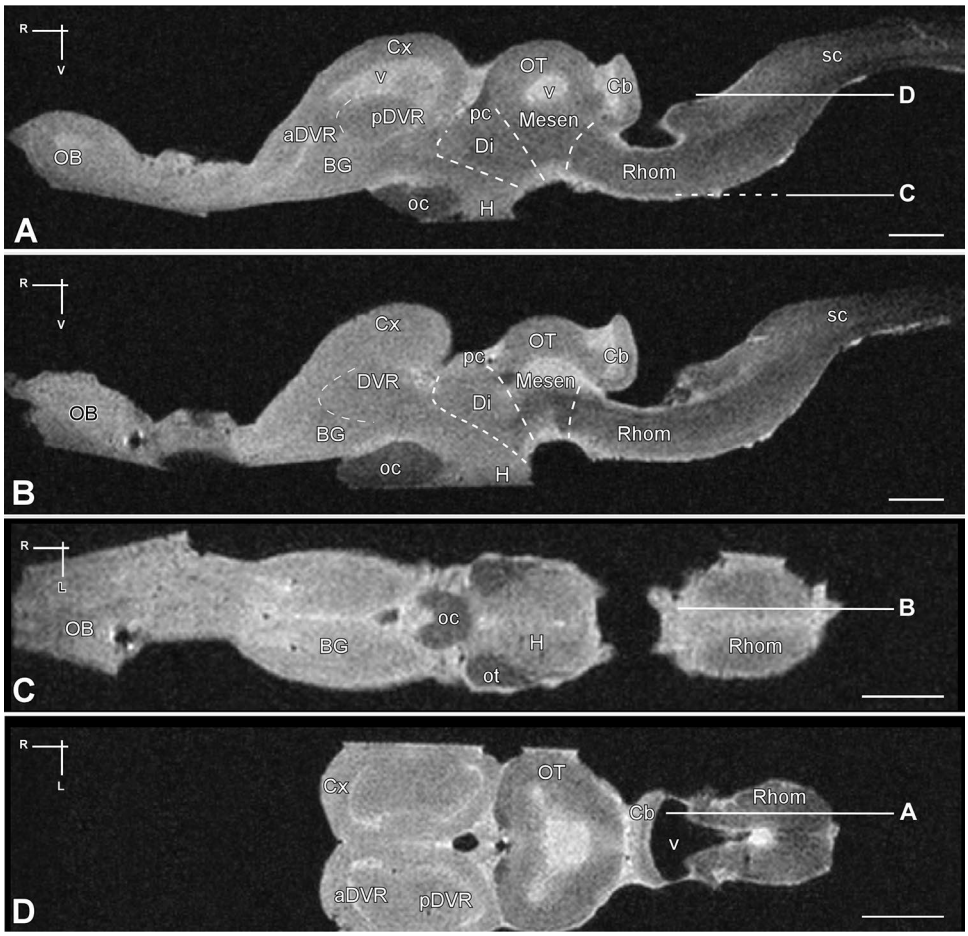

Fig. 5 Sagittal and dorsal sections of the *Pseudopus apodus* brain from 3D MRI. Sagittal (**A**, **B**) and dorsal (**C**, **D**) sections of the *Pseudopus apodus* brain with the main brain regions indicated. Scale bar = 1 mm. See the list of abbreviations for reference

were detected in the IVm nucleus and in the superficial isthmic nucleus (Iss), the isthmic reticular nucleus (Ris), and the interpeduncular nucleus (Ip; Fig. 9A, B). The isthmic complex is subdivided into a superficial portion (Iss; which is ChAT-ir), a medial 5HT-ir and CR portion (Ism; Fig. 9E, F) and a posterior portion (Isp; which is ChAT-ir; Fig. 9F). Serotonergic identification defined the raphe nuclei along caual part of the mesencephalon (Fig. 8I) and the hindbrain (Fig. 9C, D, F–I). Specifically, in the isthmic region, the combination with ChAT delineated large cells in the raphe superior nucleus (Ras), surrounding the medial longitudinal fasciculus (MLF), with significant cholinergic innervation both within the nucleus and in areas adjacent to the flm (Fig. 9D). Additional 5HT-ir cell bodies were found in a ventromedial position (Rasm; Fig. 9D). ChAT-ir cells were also identified in the interpeduncular nucleus (Ip) and fibers in the interpeduncular neuropil, originating from the retroflex fasciculus (fr; Fig. 9A–C). In the basal plate, motor neurons of the trigeminal nucleus (Vm) and the abducens nucleus (VIp) are labeled with ChAT-ir (Fig. 9F, G).

In the rhombomere 1, in the alar portion, Purkinje cells and the molecular layer of the Cb, along with the medial cerebellar nucleus (nCbm), are intensely labeled with CR-ir (Fig. 9J). Additionally, a population of CR-ir cells is observed in the corresponding parabrachial area (PB; Fig. 9J), where some TH-positive cells (Fig. 9K) are also detected. At this level, the locus coeruleus (LC) is identified by TH-ir (Fig. 9K, L). Caudally, CR-ir labels abundant fibers in the cochlear region, particularly in the lateromedial cochlear nucleus (Colm; Fig. 9M), the angularis cochlear nucleus (Coa; Fig. 9O), and the dorsomedial cochlear nucleus (Codm; Fig. 9Q). CR-ir cells are also observed in the lateroventral and medioventral vestibular nuclei (Vevl; Vevm; Fig. 9M, O, Q), as well as in the vestibulospinal tract (Vesp; Fig. 9Q, W) and the external arcuate fibers (fae; Fig. 9M). At caudal levels, separate parts of the solitary nucleus are labeled with CR and TH (Fig. 9R–V). Some TH-ir cells are found in the area postrema (ap), and CR-ir cells in the dorsal funiculus nucleus. Further caudally, in the Rhom (Fig. 9N–S), ChAT labeling identifies the ambiguous nucleus (A; Fig. 9N), which also expresses 5HT (Fig. 9N′).

Finally, in the rostral spinal cord (Fig. 9W, X), CR and TH labeling shows a population of cells in the dorsal horn, medially in laminae IV to VI, and a population of cells in contact with the cerebrospinal fluid (CSF) in TH-ir near the central canal (Fig. 9X). CR-ir fibers are observed in the

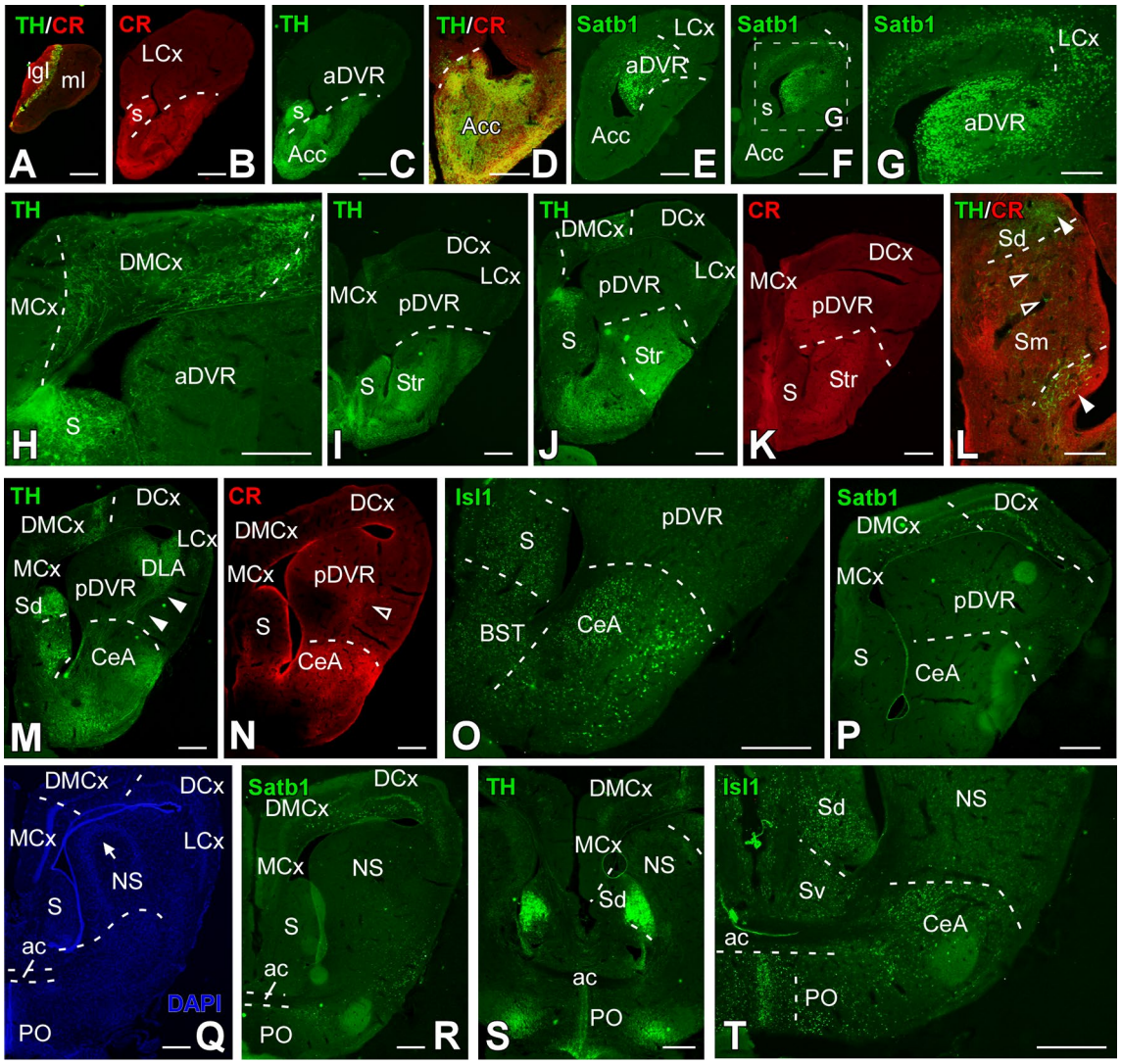

Fig. 6 Transverse sections through the telencephalic areas of the *Pseudopus apodus* brain. Photomicrographs of transverse sections through the telencephalic areas of the *Pseudopus apodus* brain, showing the distribution of specific markers in particular nuclei. The color code for the markers is provided in each image. Scale bar A–C, E, F, I–K, M, N, P–R = 500 µm; D, G, H, L, O, S, T = 200 µm. See the list of abbreviations for reference

ventral funiculus, originating from the vestibulospinal tract and the MLF.

Discussion

In recent years, the use of magnetic resonance imaging (MRI) for neuroanatomical analysis has increased significantly (Lerch et al. 2017; Heuer et al. 2019; Friedrich et al. 2021). This growth can be attributed to several factors, including the reduction in the cost of MRI techniques and the recognition by the neuroscience community of the importance of a broader approach to neurobiological modelling, enhancing studies of the evolution of the nervous system. The inclusion of a wide range of models expands the scope of knowledge, but at the same time requires careful analysis to establish new neuroanatomical and evolutionary frameworks for future research. This context has undoubtedly led to significant advances but also presents considerable challenges.

This is the primary context of our study, which provides a comprehensive neuroanatomical investigation of the brain of the legless lizard *Pseudopus apodus* using a combination of MRI, Nissl staining, and specific immunofluorescence detection of conserved markers. This research is particularly novel in that it explores a model that has been used infrequently in neuroanatomical studies, in addition, the evolutionary significance of this research is noticeable, as *Pseudopus apodus*, a

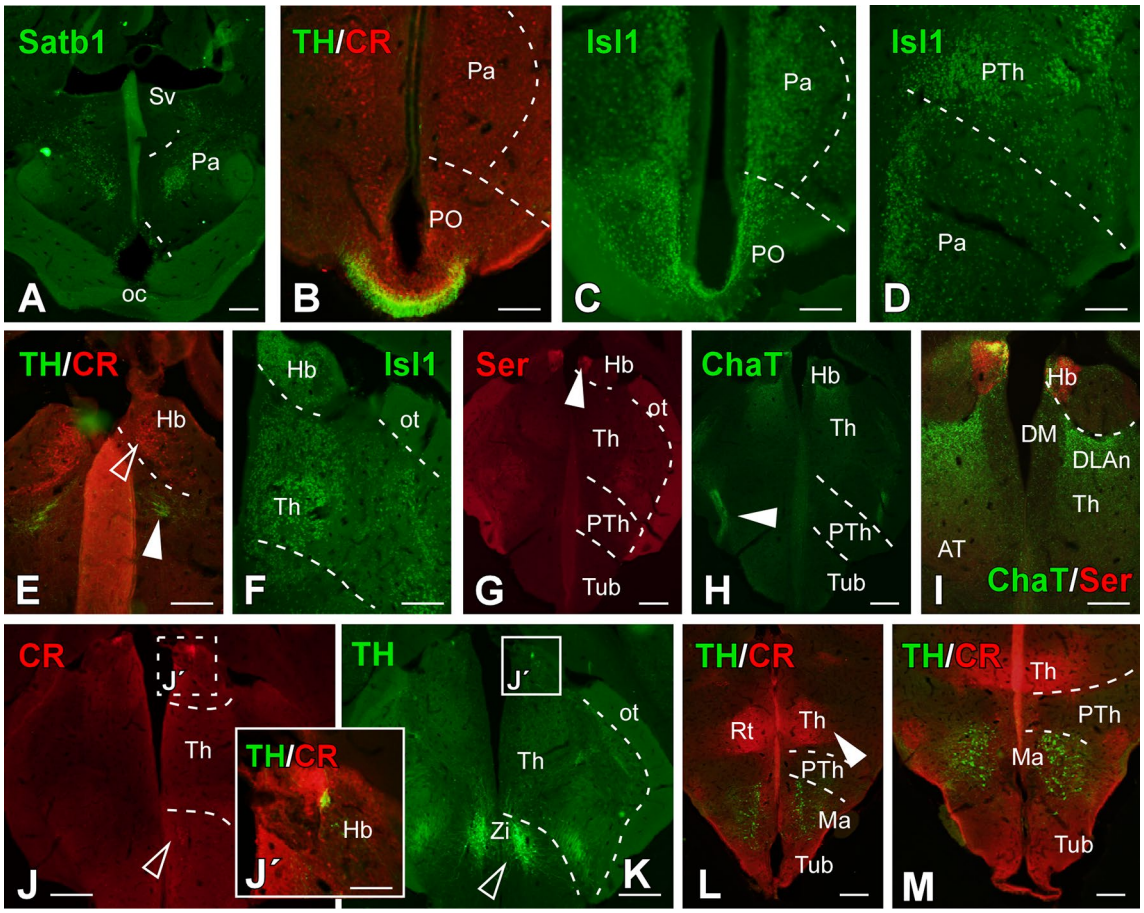

Fig. 7 Transverse sections through hypothalamic and diencephalic areas of the *Pseudopus apodus* brain. Photomicrographs of transverse sections through hypothalamic and diencephalic areas of the *Pseudopus apodus* brain, showing the distribution of specific markers in particular nuclei. The color code for the markers is provided in each image. A–F, I–K = 200 µm; G, H, L, M = 500 µm. See the list of abbreviations for reference

legless lizard, offers an exceptional model from an evolutive and comparative ecological perspective. Since the habitat preferences of *Pseudopus apodus* are diverse, reflecting its adaptability to varying geographical and environmental conditions. This species also demonstrates significant morphological plasticity, even across small geographical distances, suggesting that environmental factors such as temperature, precipitation, and predatory fauna may influence its morphological traits (Glavaš et al. 2020). This is consistent with other species exhibiting phenotypic plasticity, such as *Podarcis siculus* (Herrel et al. 2008). Thus, this model offers new insights into the organization of the lizard brain and provides a comparative analysis with existing descriptions of reptile neuroanatomy. In addition, as advances are made in the use of magnetic resonance imaging (MRI) techniques and histological analyses to study lesser-researched species, new opportunities are opening up to question established evolutionary paradigms. In this case, it is interesting to consider whether the unique neuroanatomical features of *Pseudopus apodus* constitute a window into the evolution of the neurobiology of legless reptiles, considering the morphological plasticity observed in the species.

Comparative analyses of *Pseudopus apodus* have previously focused on its anatomy, including detailed examinations of the pectoral and pelvic girdles and the hindlimbs. These studies have shown that *Pseudopus apodus* exhibits anatomical similarities with *Ophisaurus* species from North America, North Africa, and Southeast Asia (Klembara et al. 2022). Furthermore, its autapomorphic skull features clearly distinguish it from both *Anguis* and *Ophisaurus* (Klembara et al. 2017), a distinction further supported by molecular data (Jandzik et al. 2018).

In a recently published study we employed a similar methodology presenting a comparative atlas of reptilian brains, including both lizards and snakes, analyzed using MRI and nuclear labeling techniques (Jiménez et al. 2024). The data from that study, along with the findings from the current research, will be essential for distinguishing which

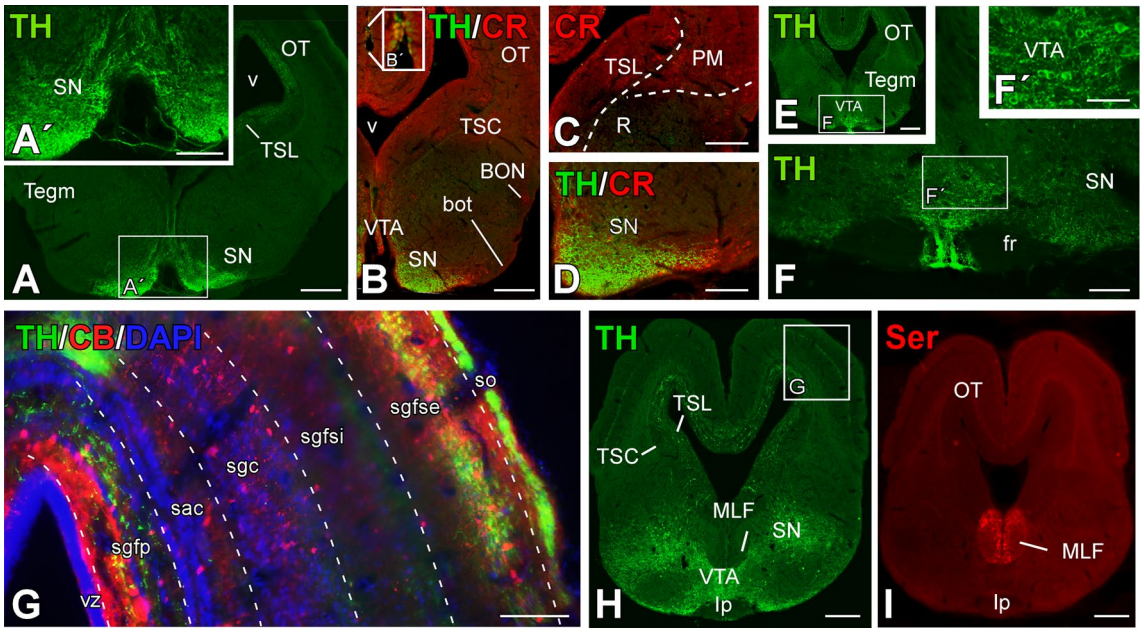

Fig. 8 Transverse sections through mesencephalic areas of the *Pseudopus apodus* brain. Photomicrographs of transverse sections through mesencephalic areas of the *Pseudopus apodus* brain, showing the distribution of specific markers in particular nuclei. The color code for the markers is provided in each image. A, B, E, H, I = 500 µm; A′, C, D, F, G = 200 µm; F′ = 100 µm. See the list of abbreviations for reference

cerebral traits are intrinsic to lizards and which are specific to snakes, independent of the functional adaptations associated with limb-lessness. Within the Anguidae family, varying degrees of limb reduction can be observed, ranging from partial reduction to complete limb-lessness. While the locomotor patterns of limbless anguilliform lizards are like those of snakes, they exhibit less developed ventral scales. In lizards, these scales play a crucial role in facilitating efficient tail-based slide-pushing locomotion, generating high lateral friction and propulsion (Spinner et al. 2015). These features underscore important distinctions between limbless anguids and snakes, highlighting their divergence from a truly tailless condition. Similarly, the brain of *Pseudopus apodus* resembles that of other lizards, with species-specific characteristics, but does not exhibit the same structural traits as those found in snakes (Jiménez et al. 2024).

MRI vs classical neuroanatomy: complementary insights and utilities in brain anatomy analysis

The application of non-invasive techniques to species that are rarely studied in research but of great scientific interest deserves further consideration, both for their usefulness to animal conservation organizations (such as zoos or wildlife rehabilitation centers) and for the valuable information they provide for comparative and evolutionary studies, providing new information for the study of neuroanatomy-function-ecology relationships. It is therefore important to determine which regions of the brain can be reliably imaged and analyzed by MRI. In addition, it also identifies at what detail or resolution they can be analyzed, as for example, MRI facilitates the visualization of large-scale brain structures, such as the dorsal ventricular crest and the nucleus accumbens, while histological analysis provides a high-resolution view of finer cellular details, such as the laminar organization of the dorsal cortex. This complementary approach highlights the inherent strengths and limitations of each technique: MRI allows observation of macroscopic structures but lacks the resolution needed to discern architecture at the cellular level, while histological techniques provide fine cellular detail but are limited by their inability to visualize large structures non-invasively.

In the rostral portion of the brain, especially in the pallium, MRI and histological analysis reveal well-organized regions, such as the dorsal and lateral cortex, although, likewise, the DVR, a key structure in reptiles involved in the processing of visual and auditory information, extends rostrocaudally and is visualized both in tissue sections and by MRI.

Regarding the regions derived from the lateral pallium in reptiles, it is important to highlight the structural differences among various taxa. Turtles exhibit a prominent nucleus known as the pallial thickening (PT), a well-defined structure that appears to be absent in lizards or reduced to only rostral regions (Jiménez et al. 2024; Desfilis et al. 2018). From a genetic and functional perspective, the PT of turtles

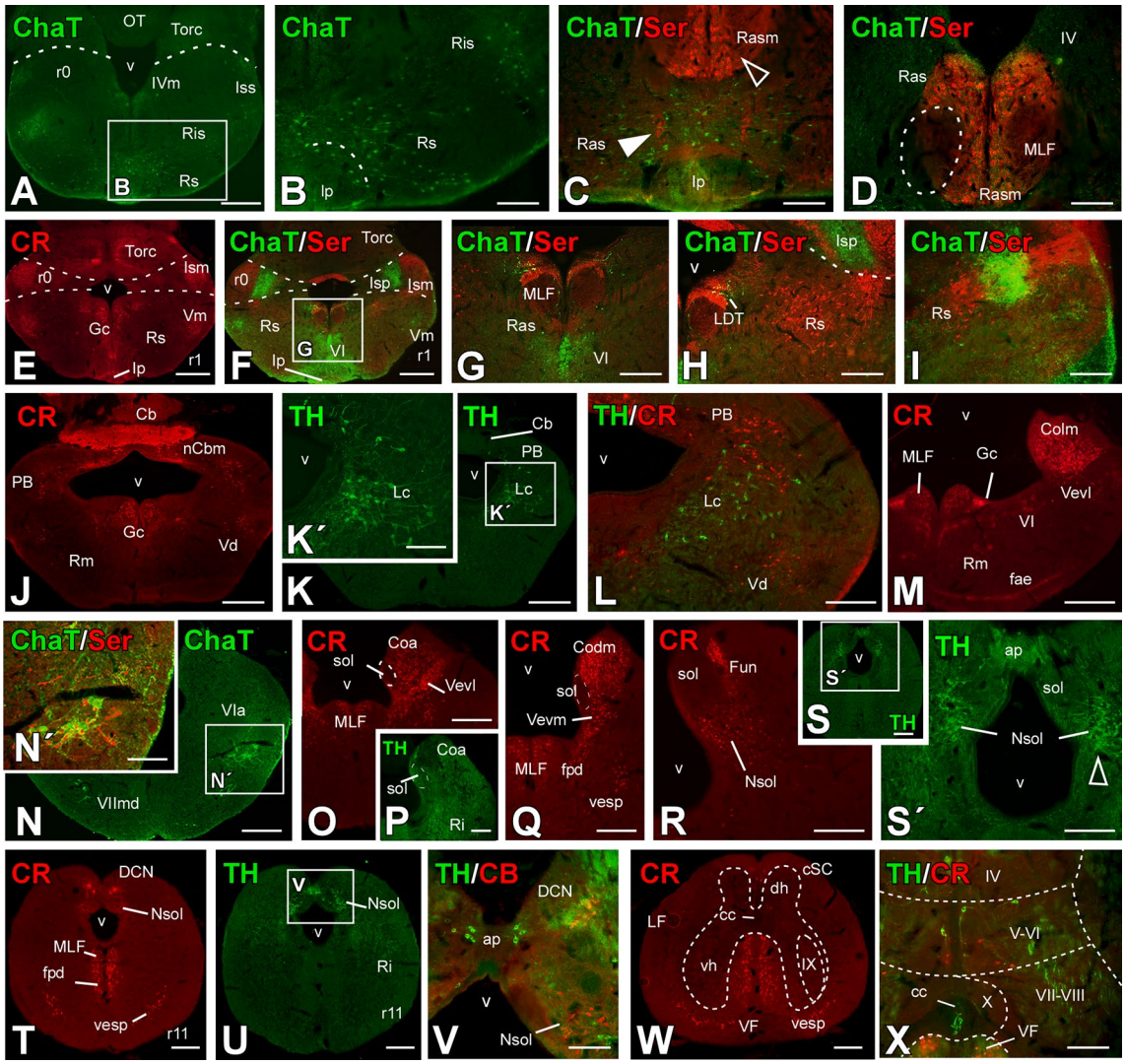

Fig. 9 Transverse sections through Isthmic, rhombencephalic and rostral spinal cord areas of the *Pseudopus apodus* brain. Photomicrographs of transverse sections through Isthmic, rhombencephalic and rostral spinal cord areas of the *Pseudopus apodus* brain, showing the distribution of specific markers in particular nuclei. The color code for the markers is provided in each image. A, E, F, J, K, M, N, O, S, T, U, W = 500 µm; B–D, G-I, K′, L, N′, P, Q, R, S′, V, X = 200 µm. See the list of abbreviations for reference

shows similarities to the anterior region of the dorsal ventricular ridge (aDVR) in *Pogona vitticeps* and to the claustrum in mammals (Schede et al. 2021; Norimoto et al. 2020; Tosches et al. 2018). Our MRI data in *P. apodus* do not allow for the identification of a distinct nucleus equivalent to the PT, in contrast to what has been observed in previous MRI studies of turtles (Jiménez et al. 2024). This finding suggests that the PT in turtles may be homologous to the aDVR of *P. apodus*, a region that we have identified through Satb1 expression, similar to what has been reported in other lizards such as *P. vitticeps* (Tosches et al. 2018) or *P. picta* (Rueda-Alaña et al. 2025), and turtles (*own results*). Further studies in *P. apodus* are necessary to determine whether this region is also involved in sleep regulation, as observed in other lizards, as well as in visual processing. The latter aspect is particularly relevant, given that the PT in turtles receives visual input from the dorsal lateral geniculate nucleus (Hall and Ebner 1970).

On the other hand, the most posterior region of the DVR (pDVR) has been identified as a multisensory integration center functionally similar to particular nuclei of the pallial amygdala in mammals. This identification is based on both its hodological characteristics (Martínez-García and Lanuza 2009) and its cellular composition (Desfilis et al. 2018; Tosches et al. 2018) and is associated with emotional behaviors such as fear (Davies et al. 2002). In this regard, we observed in *P. apodus* a TH-immunoreactive innervation extending from the basal ganglia to the lateralmost region

of the pDVR, reaching the ventricle. These amygdalostriatal projections have been previously described in reptiles (Novejarque et al. 2004). Our findings in *P. apodus* further support the hypothesis that the pDVR constitutes part of the pallial reptilian amygdala, as the presence of TH has been demonstrated in both the striatum and the developing amygdala of mammals (Bupesh et al. 2014). These data are relevant as they contribute to understanding the role of catecholaminergic neurons, whose presence in reptiles suggests their key importance in the evolution of the modulation of emotional behaviors.

Squamates, including lizards and snakes, possess a sophisticated vomeronasal chemical detection system (Schwenk 1994; Cooper Jr 1995, 1996; Filoramo and Schwenk 2009). Both groups use their tongue to sample environmental cues, transporting these chemical signals to the vomeronasal complex, located anatomically above it (Filoramo and Schwenk 2009). Beyond this common function, however, the vomeronasal system exhibits considerable variation across species, with evolutionary implications (Baeckens et al. 2017). It has been suggested that snakes exhibit the most elaborate and refined behavioral adaptations related to this sensory anatomy (Schwenk 1994). In contrast, simpler models such as iguanas possess fleshy tongues with reduced chemoreceptive capacity [*see discussion in* (Zhan et al. 2024)]. This raises an intriguing question: based on the anatomy of the tongue and vomeronasal organ (Graves and Halpern 1990; Halpern and Kubie 1983; Halpern 2007), can we infer the architecture of brain centers involved in processing these sensory inputs? and perhaps even make predictive models. The nucleus sphericus (NS), a primary secondary vomeronasal area in the squamate telencephalon (Lanuza and Halpern 1997; Martínez-Marcos et al. 2002; Martínez-Marcos and Halpern 2009), provides an ideal case for such analysis. Comparative MRI analysis is thus a valuable tool in evolutionary studies, as demonstrated in reptiles (Jiménez et al. 2024) and in *Pseudopodus* in this study. The NS is easily identifiable by MRI, allowing for the exploration of the relationships between the tongue, the vomeronasal complex, and the NS.

The diencephalic, hypothalamic, mesencephalic, and rhombencephalic regions present particular challenges for both MRI and histological analysis due to the density and complexity of the nuclei in these areas. The intricate organization of these regions complicates the distiction of specific nuclei without the use of specialized markers. However, in this respect, MRI allows a clear identification of structures such as the optic tectum, and the cerebellum, which are undoubtedly two very powerful tools of analysis at an evolutionary level. First of all, at the macro level, the anatomy of both regions in the case of *Pseudopus* is comparable to that described in other models of lizards, rather than snakes, even though they share a legless condition in both cases (ten Donkelaar 1998). And in terms of domains, the results obtained also demonstrate the conserved condition of this species with respect to other lizards, supporting that, at least in this case, the conditions of locomotor adaptation are likely to be observed at three levels, which opens an interesting question for example in the analysis of the spinal cord. Finally, MRI is effective in tracing the expansion of the ventricular system, offering important insights despite the limitations of non-specific staining and the resolution constraints of MRI in these densely populated brain regions. These findings highlight the need for further studies employing targeted marker-based approaches to achieve a more precise understanding of these complex regions.

Previous neuroanatomical studies on this model

The use of markers, neurotransmitters, neuropeptides and, in recent years, gene expression patterns as tools to define, confirm, regions and boundaries is very useful in neuroantomical studies (Puelles and Ferran 2012). The expression of neurotransmitters in the lizard brain has been analyzed in detail in recent years, although the scarcity of gene expression data in reptiles is still high. And in this context, in the case of *P. apodus*, the lack or even absence in the case of genoarchitectural analysis is total. Taking this into account, the markers used in this study, both neurotransmitters and calcium-binding proteins, as well as transcription factors, are markers widely described in other reptiles and that have been useful for the analysis of populations and/or regions and specific limits (Pierre et al. 1990; Medina et al. 1993, 1994; Guirado et al. 1999a, b; Smeets et al. 2006, 2001; Báez et al. 2003; Morona et al. 2006; Yan et al. 2010; Moreno et al. 2010, 2012; Domínguez et al. 2015; Tosches et al. 2018; Desfilis et al. 2018; Wang et al. 2021b; Hain et al. 2022; Rueda-Alaña et al. 2025). Thus, the existing neuroanatomical research on this model remains limited, with most studies dating back several decades and, in many cases, being largely inaccessible. However, extensive research has been conducted on telencephalic connectivity in reptiles, particularly lizards (Martínez-Garcia and Lanuza 2009; Lanuza et al. 2002; Hall 2008; Guirado and Dávila 2002; Bruce and Butler 1984a, b), providing much evidence for comparison. For example, connections between the septum and the medial cortex (MCx) have been documented (Belekhova and Nemova 1988), showing similarities to the hippocampal-septal connections found in all studied tetrapods (González and López 2002). Additionally, the MCx connectivity with the mammillary complex in these lizards resembles to that of mammals, supporting the idea of a homologous function (Belekhova and Kenigfest 1983). Notably, early classical anatomical studies of the medial cortex in this model established the involvement of the hippocampal-like cortex in conditioned alimentary reflexes and the dorsal ventricular

ridge in the visual processing (Ivazov 1983), suggesting a high degree of evolutionary conservation of these brain structures. Sensory input is known to reach the MCx via the medial forebrain bundle and the anterior thalamus (Belekhova and Ivazov 1983) and notably, the thalamus also exhibits conserved features, such as GABA expression in the dorsal lateral geniculate nucleus (Rio et al. 1992) and the established connections between the ventral lateral geniculate nucleus and the hypothalamus (Belekhova 1991). Additionally, TH-positive innervations can be observed in the dorsomedial cortex of *P. apodus*, similar to what occurs in the cornu ammonis 3 (CA3) region of mammals (Milner and Bacon 1989). This finding provides further evidence of the homology between mammal-hippocampus and reptile-MCx/DMCx (Reiter et al. 2017).

The neurochemistry of the lizard brain has been extensively explored, leading to the identification of its primary subdivisions and enabling evolutive comparisons with other reptiles and amniotes (Medina et al. 1993; Báez et al. 2003; Tosches et al. 2018; Desfilis et al. 2018; Hain et al. 2022; Wang et al. 2021a). However, research focusing specifically on apoda lizards remains relatively scarce. The analysis of specific markers, such as Satb1, CR, 5HT and TH has significantly advanced our understanding of the brain regions. For instance, high levels of Satb1 expression in the anterior dorsal ventricular ridge (aDVR) allow for clear delineation of this rostral region from the more caudal part of the DVR, which does not exhibit Satb1 expression. Similarly, distinct staining patterns in the nucleus accumbens, dorsal cortex, and thalamic regions contribute to their anatomical identification. Furthermore, serotonin expression in the brain of this model closely mirrors that observed in other lizards (Pierre et al. 1990). In summary, the application of these markers not only corroborates previous findings in reptilian neuroanatomy but also offers novel insights into the organization of brain regions in *Pseudopus apodus*, contributing to a more refined understanding of its neural architecture.

Acknowledgements The authors thank Juncal Fernández-Garayzábal for her help in editing this manuscript.

Author contributions All authors have read and agreed to the published version of the manuscript. Conceptualization: G-SJ. and MN. Histology and inmunofluorescence analysis: JS. Magnetic resonance imaging: R-FM-J, G-RMI., FV., CD. Data analysis: JS., MR. and MN. Writing—original draft preparation: JS., RM., G-SJ. and MN. Writing—review and editing, G-SJ. and MN. Funding acquisition: G-SJ. and NM.

Funding Open Access funding provided thanks to the CRUE-CSIC agreement with Springer Nature. This research was supported by funding from the Complutense University of Madrid (Innova Project UCM No. 379) and Spanish Ministry of Science and Innovation, Grant/Award Number: PID2023-147228 NB-I00.

Data availability The rows of all models are not publicly available due to privacy reasons but are available upon request to the corresponding author.

Declarations

Conflict of interest The authors declare no conflicts of interest.

Ethical approval The original research reported herein was performed according to the regulations and laws established by European Union (2010/63/EU) and Spain (Royal Decree 1386/2018) for care and handling of animals in research and after approval from the Complutense University to conduct the experiments described ((O.H. (CEA)- UCM-NP0409032022-2022).

References

Arnold N, Ovenden D (2002) Reptiles and amphibians of Europe. Princeton University Press

Baeckens S, Herrel A, Broeckhoven C, Vasilopoulou-Kampitsi M, Huyghe K, Goyens J, Van Damme R (2017) Evolutionary morphology of the lizard chemosensory system. Sci Rep 7(1):10141

Báez J, Monzón-Mayor M, Yanes C, del Mar R-A, Francisco Arbelo-Galván J, Puelles L (2003) Neuronal differentiation patterns in the optic tectum of the lizard *Gallotia galloti*. Brain Res 975(1–2):48–65. https://doi.org/10.1016/s0006-8993(03)02586-1

Behroozi M, Billings BK, Helluy X, Manger PR, Güntürkün O, Ströckens F (2018) Functional MRI in the Nile crocodile: a new avenue for evolutionary neurobiology. Proc R Soc B Biol Sci 285(1877):20180178

Belekhova M (1990) Connections linking the mamillary complex and hypothalamo-tegmental area of the brain with the brainstem in lizards. Neurophysiology 22(1):95–102

Belekhova M (1991) Geniculo-and subthalamohypothalamic connections in the lizard: HRP study. J Hirnforsch 32(1):55–59

Belekhova M, Ivazov N (1983) Analysis of the conduction of visual, somatic and audiovibrational sensory information of the hippocampal cortex in the lizard. Neirofiziologiia = Neurophysiology 15(2):153–160

Belekhova M, Kenigfest N (1983) Study of the connections of the hippocampal (mediodorsal) cortex of *Ophisaurus apodus* by means of horseradish peroxidase axonal transport. Neiřofiziologiia 15:145

Belekhova M, Nemova G (1987) Study of connections of supposed limbic diencephalic nuclei in lizards using axonic HRP transport. Neurofiziol 19:110–120

Belekhova M, Nemova G (1988) Study of septal connections in lizards using axonal HRP transport. Neirofiziologia 20:398–407

Bruce LL, Butler AB (1984a) Telencephalic connections in lizards. I. Projections to cortex. J Comp Neurol 229(4):585–601. https://doi.org/10.1002/cne.902290411

Bruce LL, Butler AB (1984b) Telencephalic connections in lizards. II. Projections to anterior dorsal ventricular ridge. J Comp Neurol 229(4):602–615. https://doi.org/10.1002/cne.902290412

Bupesh M, Vicario A, Abellán A, Desfilis E, Medina L (2014) Dynamic expression of tyrosine hydroxylase mRNA and protein in neurons of the striatum and amygdala of mice, and experimental evidence of their multiple embryonic origin. Brain Struct Funct 219(3):751–776. https://doi.org/10.1007/s00429-013-0533-7

Çiçek K, Tok CV, Hayretdağ S, Ayaz D (2014) Data on the Food Composition of European Glass Lizard, Pseudopus apodus (Pallas, 1775) (Squamata: Anguidae) from Çanakkale (Western Anatolia, Turkey). Acta Zool Bulg 66(3):433–436

Cooper WE Jr (1995) Foraging mode, prey chemical discrimination, and phylogeny in lizards. Anim Behav 50(4):973–985

Cooper WE Jr (1996) Chemosensory recognition of familiar and unfamiliar conspecifics by the scincid lizard *Eumeces laticeps*. Ethology 102(3):454–464

Davies DC, Martínez-García F, Lanuza E, Novejarque A (2002) Striato-amygdaloid transition area lesions reduce the duration of tonic immobility in the lizard *Podarcis hispanica*. Brain Res Bull 57(3–4):537–541. https://doi.org/10.1016/s0361-9230(01)00687-6

Desfilis E, Abellán A, Sentandreu V, Medina L (2018) Expression of regulatory genes in the embryonic brain of a lizard and implications for understanding pallial organization and evolution. J Comp Neurol 526(1):166–202. https://doi.org/10.1002/cne.24329

Domínguez L, González A, Moreno N (2015) Patterns of hypothalamic regionalization in amphibians and reptiles: common traits revealed by a genoarchitectonic approach. Front Neuroanat 9:3. https://doi.org/10.3389/fnana.2015.00003

Filoramo NI, Schwenk K (2009) The mechanism of chemical delivery to the vomeronasal organs in squamate reptiles: a comparative morphological approach. J Exp Zool A Ecol Genet Physiol 311(1):20–34

Friedrich P, Forkel SJ, Amiez C, Balsters JH, Coulon O, Fan L, Goulas A, Hadj-Bouziane F, Hecht EE, Heuer K (2021) Imaging evolution of the primate brain: the next frontier? Neuroimage 228:117685

García-Real MI, Fernández-Valle E, Jiménez S, Ruiz-Fernández MJ, Castejón-Ferrer D, Montesinos-Barceló A, Ardiaca-García M, Moreno N, González-Soriano J (2025) *Pseudopus apodus* soft tissue anatomy based on comparison of classical dissection and multi-detector computed tomography. Animals 15(5):615

Glavaš OJ, Počanić P, Lovrić V, Derežanin L, Tadić Z, Lisičić D (2020) Morphological and ecological divergence in two populations of European glass lizard, *Pseudopus apodus* (Squamata: Anguidae). Zool Res 41(2):172

González A, López JM (2002) A forerunner of septohippocampal cholinergic system is present in amphibians. Neurosci Lett 327(2):111–114

Graves BM, Halpern M (1990) Roles of vomeronasal organ chemoreception in tongue flicking, exploratory and feeding behaviour of the lizard, *Chalcides ocellatus*. Anim Behav 39(4):692–698. https://doi.org/10.1016/S0003-3472(05)80380-X

Guirado S, Dávila JC (2002) Thalamo-telencephalic connections: new insights on the cortical organization in reptiles. Brain Res Bull 57(3):451–454. https://doi.org/10.1016/S0361-9230(01)00677-3

Guirado S, Dávila JC, Real MA, Medina L (1999a) Nucleus accumbens in the lizard *Psammodromus algirus*: chemoarchitecture and cortical afferent connections. J Comp Neurol 405(1):15–31. https://doi.org/10.1002/(sici)1096-9861(19990301)405:1%3c15::aid-cne2%3e3.0.co;2-v

Guirado S, Martínez-García F, Andreu MJ, Dávila JC (1999b) Calcium-binding proteins in the dorsal ventricular ridge of the lizard *Psammodromus algirus*. J Comp Neurol 405(1):32–44. https://doi.org/10.1002/(sici)1096-9861(19990301)405:1%3c32::aid-cne3%3e3.0.co;2-z

Hain D, Gallego-Flores T, Klinkmann M, Macias A, Ciirdaeva E, Arends A, Thum C, Tushev G, Kretschmer F, Tosches MA, Laurent G (2022) Molecular diversity and evolution of neuron types in the amniote brain. Science 377(6610):eabp8202. https://doi.org/10.1126/science.abp8202

Hall WC (2008) Visual pathways to the telencephalon in reptiles and mammals. Brain Behav Evol 5(2–3):95–113. https://doi.org/10.1159/000123741

Hall WC, Ebner FF (1970) Parallels in the visual afferent projections of the thalamus in the hedgehog (*Paraechinus hypomelas*) and the turtle (*Pseudemys scripta*). Brain Behav Evol 3(1):135–154. https://doi.org/10.1159/000125467

Halpern M (2007) 2.18 - The evolution of the vomeronasal system. In: Kaas JH (ed) Evolution of nervous systems. Academic Press, Oxford, pp 407–415

Halpern M, Kubie JL (1983) Snake tongue flicking behavior: clues to vomeronasal system functions. In: Müller-Schwarze D, Silverstein RM (eds) Chemical signals in vertebrates 3. Springer US, Boston, MA, pp 45–72

Herrel A, Huyghe K, Vanhooydonck B, Backeljau T, Breugelmans K, Grbac I, Van Damme R, Irschick DJ (2008) Rapid large-scale evolutionary divergence in morphology and performance associated with exploitation of a different dietary resource. Proc Natl Acad Sci 105(12):4792–4795. https://doi.org/10.1073/pnas.0711998105

Heuer K, Gulban OF, Bazin P-L, Osoianu A, Valabregue R, Santin M, Herbin M, Toro R (2019) Evolution of neocortical folding: a phylogenetic comparative analysis of MRI from 34 primate species. Cortex 118:275–291

Hoffmann R, Schultz J, Schellhorn R, Rybacki E, Keupp H, Gerden SR, Lemanis R, Zachow S (2014) Non-invasive imaging methods applied to neo- and paleo-ontological cephalopod research. Biogeosciences 11:2721–2739. https://doi.org/10.5194/bg-11-2721-2014

Hoops D, Desfilis E, Ullmann JF, Janke AL, Stait-Gardner T, Devenyi GA, Price WS, Medina L, Whiting MJ, Keogh JS (2018) A 3D MRI-based atlas of a lizard brain. J Comp Neurol 526(16):2511–2547

Hoops D, Weng H, Shahid A, Skorzewski P, Janke AL, Lerch JP, Sled JG (2021) A fully segmented 3D anatomical atlas of a lizard brain. Brain Struct Funct 226(6):1727–1741

Ivazov NI (1983) Role of the hippocampal cortex and dorsal ventricular ridge in conditioned reflex activity of the anguid lizard scheltopusik (*Ophisaurus apodue*). Neurosci Behav Physiol 13(6):397–403. https://doi.org/10.1007/BF01182680

Ivazov N, Belekhova M (1982) Electrophysiological studies on afferent organization of the thalamus in the lizard *Ophisaurus apodus*. J Evol Biochem Physiol 18:76–86

Jandzik D, Jablonski D, Zinenko O, Kukushkin OV, Moravec J, Gvoždík V (2018) Pleistocene extinctions and recent expansions in an anguid lizard of the genus Pseudopus. Zool Scr 47(1):21–32. https://doi.org/10.1111/zsc.12256

Jiménez S, Santos-Álvarez I, Fernández-Valle E, Castejón D, Villa-Valverde P, Rojo-Salvador C, Pérez-Llorens P, Ruiz-Fernández MJ, Ariza-Pastrana S, Martín-Orti R (2024) Comparative MRI analysis of the forebrain of three sauropsida models. Brain Struct Funct 229(6):1349–1364

Jiménez S, Senovilla-Ganzo R, Gallego-Flores T, Pérez-Pascual E, Ordeñana-Manso A, Rayo-Morales R, De Pittà M, García-Moreno F (2025) Experimental neurogenesis in the embryos of the gecko *Paroedura picta*. Methods Mol Biol 2899:127–145. https://doi.org/10.1007/978-1-0716-4386-0_9

Klembara J (2015) New finds of anguines (Squamata, Anguidae) from the Early Miocene of Northwest Bohemia (Czech Republic). Paläontol Z 89:171–195

Klembara J, Dobiašová K, Hain M, Yaryhin O (2017) Skull anatomy and ontogeny of legless lizard *Pseudopus apodus* (Pallas, 1775): heterochronic influences on form. Anat Rec (Hoboken) 300(3):460–502. https://doi.org/10.1002/ar.23532

Klembara J, Yaryhin O, Majerová J, Hain M (2022) Comparative anatomy and ontogeny of appendicular skeleton of *Pseudopus apodus* (Pallas, 1775) (Anguimorpha, Anguidae) and a pattern of hindlimb loss in Anguinae. Anat Rec (Hoboken) 305(9):2290–2311. https://doi.org/10.1002/ar.24851

Kukushkin OV, Dovgal IV (2018) Sexual dimorphism in *Pseudopus apodus* (Reptilia: Sauria: Anguidae) from the Steppe Crimea. Ecol Montenegrina 19:1–21

Kulikov G, Safarov KM (1969) Afferent systems in the fore-and mid-brain in lizards (*Ophisaurus apus*). Dokl Akad Nauk SSSR 187(4):952–955

Lanuza E, Halpern M (1997) Afferent and efferent connections of the nucleus sphericus in the snake *Thamnophis sirtalis*: convergence of olfactory and vomeronasal information in the lateral cortex and the amygdala. J Comp Neurol 385(4):627–640. https://doi.org/10.1002/(sici)1096-9861(19970908)385:4%3c627::aid-cne8%3e3.0.co;2-5

Lanuza E, Novejarque A, Moncho-Bogani J, Hernández A, Martínez-García F (2002) Understanding the basic circuitry of the cerebral hemispheres: the case of lizards and its implications in the evolution of the telencephalon. Brain Res Bull 57(3):471–473. https://doi.org/10.1016/S0361-9230(01)00710-9

Lerch JP, van der Kouwe AJW, Raznahan A, Paus T, Johansen-Berg H, Miller KL, Smith SM, Fischl B, Sotiropoulos SN (2017) Studying neuroanatomy using MRI. Nat Neurosci 20(3):314–326. https://doi.org/10.1038/nn.4501

Macey JR, Schulte JA II, Larson A, Tuniyev BS, Orlov N, Papenfuss TJ (1999) Molecular phylogenetics, tRNA evolution, and historical biogeography in anguid lizards and related taxonomic families. Mol Phylogenet Evol 12(3):250–272

Martínez-García F, Lanuza E (2009) Evolution of association pallial areas. in reptiles. In: Binder MD, Hirokawa N, Windhorst U (eds) Encyclopedia of neuroscience. Springer, Berlin, pp 1219–1225

Martínez-Marcos A, Halpern M (2009) Evolution of olfactory and vomeronasal systems. In: Binder MD, Hirokawa N, Windhorst U (eds) Encyclopedia of neuroscience. Springer, Berlin, pp 1264–1269

Martínez-Marcos A, Lanuza E, Halpern M (2002) Neural substrates for processing chemosensory information in snakes. Brain Res Bull 57(3):543–546. https://doi.org/10.1016/S0361-9230(01)00686-4

Medina L, Smeets WJ, Hoogland PV, Puelles L (1993) Distribution of choline acetyltransferase immunoreactivity in the brain of the lizard *Gallotia galloti*. J Comp Neurol 331(2):261–285. https://doi.org/10.1002/cne.903310209

Medina L, Puelles L, Smeets WJ (1994) Development of catecholamine systems in the brain of the lizard *Gallotia galloti*. J Comp Neurol 350(1):41–62. https://doi.org/10.1002/cne.903500104

Mietchen D, Aberhan M, Manz B, Hampe O, Mohr B, Neumann C, Volke F (2007) Three-dimensional magnetic resonance imaging of fossils across taxa. Biogeosci Discuss 4(4):2959–3004

Milner TA, Bacon CE (1989) Ultrastructural localization of tyrosine hydroxylase-like immunoreactivity in the rat hippocampal formation. J Comp Neurol 281(3):479–495. https://doi.org/10.1002/cne.902810311

Moreno N, Morona R, López JM, González A (2010) Subdivisions of the turtle *Pseudemys scripta* subpallium based on the expression of regulatory genes and neuronal markers. J Comp Neurol 518(24):4877–4902. https://doi.org/10.1002/cne.22493

Moreno N, Domínguez L, Morona R, González A (2012) Subdivisions of the turtle *Pseudemys scripta* hypothalamus based on the expression of regulatory genes and neuronal markers. J Comp Neurol 520(3):453–478. https://doi.org/10.1002/cne.22762

Morona R, López JM, González A (2006) Calbindin-D28k and calretinin immunoreactivity in the spinal cord of the lizard *Gekko gecko*: colocalization with choline acetyltransferase and nitric oxide synthase. Brain Res Bull 69(5):519–534. https://doi.org/10.1016/j.brainresbull.2006.02.022

Norimoto H, Fenk LA, Li H-H, Tosches MA, Gallego-Flores T, Hain D, Reiter S, Kobayashi R, Macias A, Arends A (2020) A claustrum in reptiles and its role in slow-wave sleep. Nature 578(7795):413–418

Novejarque A, Lanuza E, Martínez-García F (2004) Amygdalostriatal projections in reptiles: a tract-tracing study in the lizard *Podarcis hispanica*. J Comp Neurol 479(3):287–308. https://doi.org/10.1002/cne.20309

Obst FJ (1978) Zur geographischen Variabilität des Scheltopusik, *Ophisaurus apodus* (Pallas). Zool Abh Staat Mus Tierk Dresden 35:129–140

Obst FJ (1981) *Ophisaurus apodus* (Pallas, 1775)-Scheltopusik. In: Handbuch der Reptilien und Amphibien Europas. Echsen (Sauria). Akademische Verlags gesellschaft, Wiesbaden, vol 1, pp 259–274

Oelschläger HHA, Haas-Rioth M, Fung C, Ridgway SH, Knauth M (2007) Morphology and evolutionary biology of the dolphin (*Delphinus* sp.) brain – MR imaging and conventional histology. Brain Behav Evol 71(1):68–86. https://doi.org/10.1159/000110495

Pallas P (1775) Lacerta apoda descripta. Novi Comment Acad Sci Imp Petropol 19:435–454

Pierre J, Reperant J, Belekhova M, Nemova L, Vesselkin N, Miceli D (1990) Immunohistochemical analysis of the serotonin system in the brain of lizard *Ophisaurus apodus*. C R Acad Sci 311(1):43–49

Pritz MB, Ziegler LC, Thompson TN, Hsu EW (2020) Magnetic resonance diffusion tensor tractography of a midbrain auditory circuit in Alligator. Neurosci Lett 738:135251

Puelles L, Ferran JL (2012) Concept of neural genoarchitecture and its genomic fundament. Front Neuroanat 6:47. https://doi.org/10.3389/fnana.2012.00047

Pyron RA, Burbrink FT, Wiens JJ (2013) A phylogeny and revised classification of Squamata, including 4161 species of lizards and snakes. BMC Evol Biol 13(1):93. https://doi.org/10.1186/1471-2148-13-93

Reiter S, Liaw H-P, Yamawaki TM, Naumann RK, Laurent G (2017) On the value of reptilian brains to map the evolution of the hippocampal formation. Brain Behav Evol 90(1):41–52. https://doi.org/10.1159/000478693

Rifai L, Baker M, Shafei DA, Disi A, Mahasneh A, Amr Z (2005) *Pseudopus apodus* (PALLAS, 1775) from Jordan, with notes on its ecology. Herpetozoa 18(3/4):133–140

Rio J-P, Repérant J, Ward R, Miceli D, Medina M (1992) Evidence of GABA-immunopositive neurons in the dorsal part of the lateral geniculate nucleus of reptiles: morphological correlates with interneurons. Neuroscience 47(2):395–407

Rueda-Alaña E, Senovilla-Ganzo R, Grillo M, Vázquez E, Marco-Salas S, Gallego-Flores T, Ordeñana-Manso A, Ftara A, Escobar L, Benguría A, Quintas A, Dopazo A, Rábano M, Vivanco MD, Aransay AM, Garrigos D, Toval Á, Ferrán JL, Nilsson M, Encinas-Pérez JM, De Pittà M, García-Moreno F (2025) Evolutionary convergence of sensory circuits in the pallium of amniotes. Science 387(6735):eadp3411. https://doi.org/10.1126/science.adp3411

Schede HH, Schneider CG, Stergiadou J, Borm LE, Ranjak A, Yamawaki TM, David FPA, Lönnerberg P, Tosches MA, Codeluppi S, La Manno G (2021) Spatial tissue profiling by imaging-free molecular tomography. Nat Biotechnol 39(8):968–977. https://doi.org/10.1038/s41587-021-00879-7

Schwenk K (1994) Why snakes have forked tongues. Science 263(5153):1573–1577

Smeets WJ, Lopez JM, González A (2001) Immunohistochemical localization of DARPP-32 in the brain of the lizard, *Gekko gecko*: co-occurrence with tyrosine hydroxylase. J Comp Neurol 435(2):194–210. https://doi.org/10.1002/cne.1202

Smeets WJ, López JM, González A (2006) Distribution of neuropeptide FF-like immunoreactivity in the brain of the lizard *Gekko gecko* and its relation to catecholaminergic structures. J Comp Neurol 498(1):31–45. https://doi.org/10.1002/cne.21035

Spinner M, Bleckmann H, Westhoff G (2015) Morphology and frictional properties of scales of *Pseudopus apodus* (Anguidae, Reptilia). Zoology 118(3):171–175. https://doi.org/10.1016/j.zool.2014.11.002

ten Donkelaar HJ (1998) Reptiles. In: Nieuwenhuys R, ten Donkelaar HJ, Nicholson C (eds) The central nervous system of vertebrates: volume 1/, volume 2/, volume 3. Springer, Berlin, pp 1315–1524

Tosches MA, Yamawaki TM, Naumann RK, Jacobi AA, Tushev G, Laurent G (2018) Evolution of pallium, hippocampus, and cortical cell types revealed by single-cell transcriptomics in reptiles. Science 360(6391):881–888

Vickery S, Hopkins WD, Sherwood CC, Schapiro SJ, Latzman RD, Caspers S, Gaser C, Eickhoff SB, Dahnke R, Hoffstaedter F (2020) Chimpanzee brain morphometry utilizing standardized MRI preprocessing and macroanatomical annotations. Elife. https://doi.org/10.7554/eLife.60136

Wang X-Q, Wang W-B, Tang Y-Z, Dai Z-D (2021a) Subdivisions of the mesencephalon and isthmus in the lizard as revealed by ChAT immunohistochemistry. Anat Rec 304(9):2014–2031. https://doi.org/10.1002/ar.24595

Wang XQ, Wang WB, Tang YZ, Dai ZD (2021b) Subdivisions of the mesencephalon and isthmus in the lizard Gekko gecko as revealed by ChAT immunohistochemistry. Anat Rec (Hoboken) 304(9):2014–2031. https://doi.org/10.1002/ar.24595

Yan K, Tang YZ, Carr CE (2010) Calcium-binding protein immunoreactivity characterizes the auditory system of *Gekko gecko*. J Comp Neurol 518(17):3409–3426. https://doi.org/10.1002/cne.22428

Zhan L, Chen Y, He J, Guo Z, Wu L, Storey KB, Zhang J, Yu D (2024) The phylogenetic relationships of major lizard families using mitochondrial genomes and selection pressure analyses in anguimorpha. Int J Mol Sci. https://doi.org/10.3390/ijms25158464